COMMUN. MATH. SCI.
Vol. 17, No. 5, pp. 1427–1436

AN OPTIMIZATION PRINCIPLE FOR INITIATION AND ADAPTATION OF BIOLOGICAL TRANSPORT NETWORKS*

DAN HU† AND DAVID CAI‡

In memory of Professor David Shenou Cai

Abstract. Structural optimization of biological transport networks, such as leaf venation and blood vessel systems, can be regarded as a consequence of natural selection. Many studies have examined the important question of whether an adaptation dynamics of edges can be responsible for structural optimization. However, what role the initiation process plays in structural optimization remains to be clarified. Here we propose an optimization principle that potentially underlies common mechanisms that drive the formation of biological transport networks. Associated with the optimization principle is an adaptation dynamics of cell polarization that unifies initiation processes and segment formation of transport networks. In our model, the competition between the reduction of transport energy cost and the reduction of material and metabolic consumptions is sufficient to induce optimal structures: a tree-like network as well as loops under different states of fluctuating drives.

Keywords. Biological Transport Networks; initiation, adaptation.

AMS subject classifications. 60F10; 60J75; 62P10; 92C37.

1. Introduction

Efficient and robust transport networks are the cornerstone of our modern industrial life for quick delivery of people, goods, energy, and information. Despite their importance, a clear global designing principle of such networks is not present to guarantee their efficiency and robustness in general [1]. In fact, the large scale structure of most industrial transport networks results from adaptive construction in response to continuous changing local requirements. One may be interested in how good the global efficiency of such a local adaptive strategy can be in constructing transport networks. Many transport networks, such as railway and highway networks, are naturally embedded in two- or three-dimensional spaces. It is also of interest to study the strategy of introducing such geometrical constraints in network designing. Furthermore, as suggested by idealized models, such as the Steiner tree model [1–3], non-convex optimization and multiple solutions may generally exist in the designing of transport networks. It is important to study the way of avoiding high cost solutions in real applications.

Transport networks such as blood vessel systems and leaf venations also play a crucial role in nutrient supply and waste removal for large life systems. As a consequence of natural selection, one may simply believe that a kind of structural optimization for biological transport networks, tailored for their physiological demanding and geometrical constraints (such as the two-dimensional structure of leaves and retina), has been selected by the long evolution history. An important scientific question is: do there exist macroscopic principles in general that control and organize underlying biochemical and physiological processes of biological transport networks? A deep exploration of this question may provide understandings in twofold – (1) the relatively simple macroscopic function of the complex high-dimensional microscopic biological processes in the con-

*Received: May, 12, 2018; Accepted (in revised form): April 4, 2019.

†School of Mathematical Sciences, Institute of Natural Sciences, and MOE-LSC, Shanghai Jiao Tong University, Shanghai, 200240, China (hudan80@sjtu.edu.cn). http://ins.sjtu.edu.cn/people/dhu.

‡School of Mathematical Sciences, Institute of Natural Sciences, and MOE-LSC, Shanghai Jiao Tong University, Shanghai, 200240, China; Courant Institute and Center for Neural Science, New York University, New York, NY10012, U.S.A; NYUAD Institute, New York University Abu Dhabi, PO Box 129188, Abu Dhabi, UAE.

struction of biological transport networks and (2) a bionic means of designing efficient and robust transport networks under geometrical constraints.

There has been a long interest in the designing principle of biological transport networks, including the scaling properties of the blood vessel diameters and the origin of specific network structures. Experimental studies have shown that for small blood vessels, there is an approximate cubic law, $D^3 = D_l^3 + D_r^3$, between the diameter D of a parent vessel and the diameters D_l and D_r of its daughter vessels [4]. By optimization of the total energy cost in blood flow delivery and metabolic cost of blood cells, Murray successfully explained this cubic relation, consequently, suggesting that there is a narrow range of wall shear stress of the blood flow [5]. Biological transport networks that contain many loops while maintaining an impression of a tree-like major structure are believed to afford great benefits to living systems, including energy efficiency [1,6–16], mechanical robustness [17], and damage tolerance [8]. With given initial network geometry, it is shown that adaptation dynamics of network edges in response to local stimuli, such as the adaptation of blood vessel diameters in response to the wall shear stress of blood flow, can lead to structural optimization [13–16].

The mechanisms for initiation of transport networks has been under active explorations. Experimental studies have drawn attention to the importance of hormone transport for initiating a biological transport network in both animals and plants. It has been shown that for embryo vasculogenesis [18], the network of endothelial cells is initiated before the heart starts to beat, eventually forming the earliest circulation system. During leaf budding [19–22], it has been observed that delivery of auxin is concentrated on a "network" of cells with an enhanced power of active transport, which eventually develops to form the leaf venation. Theoretically, it has also been demonstrated that migration and elongation of endothelial cells driven by chemoattractants may be essential in vasculogenesis and angiogenesis [23, 24]. Canalization was hypothesized [20, 22, 25–28] to stress the role of auxin in the formation of leaf veins, that is, the differentiation of cells induced by transport of auxin enhances its power in active transport. Furthermore, pruning of unnecessary blood vessels has been observed as sequential events of vessel adaptation to optimize the network structure [14–16].

Although the endothelial cells of pruned vessels can migrate to be reused elsewhere [14], signal pathways that can reduce the frequency of vessel pruning in vasculogenesis and angiogenesis may significantly reduce energy cost in the formation of blood vessel systems. For plants whose vascular cells cannot move freely, a pruning process is not efficient and it is of particular importance to find optimal networks of low energy cost through the initiation process. However, the important question of what is the role of the initiation process remains to be elucidated in structural optimization of biological transport networks. A governing principle that can incorporate the initiation process in structural optimization may shed light on the global effects of signal pathways on the initiation process of biological transport networks.

In this work, we propose an optimization process as an organization principle underlying the physiological mechanism of the initiation process. We address the question of what are the characteristics of intrinsically required driving stimuli and their physiological function in the initiation process of biological transport networks; what role the initiation process can play in the optimization of the network structure; and what is the mechanism underlying the initial formation of loops in a network. Based on our model and simulation results, we also discuss possible bionic means of designing efficient and robust transport networks, which can be naturally embedded in two- or three-dimensional spaces.

2. Mathematical modeling of the initiation and adaptation process of biological transport networks

We hypothesize that as a result of the long evolution history, the total effective energy cost function of biological transport networks is optimized by reducing the mechanical energy cost in transport and metabolic energy cost in forming the network. We use this optimization principle to construct a continuum model to incorporate both the initiation and adaptation processes of biological transport networks. Our continuum model does not require a preexisting network structure and in this model the optimal transport network can naturally emerge.

In our model, we include the three transport means in tissue – pure diffusion, active transport, and flow in veins. As can be seen from the experiment on leaf budding [19–22], the active transport of auxin can concentrate on a specific direction as a result of a direction-specific line-up of transmembrane proteins. To describe the enhancement of active transport, we use the polarization vector, $\mathbf{m}$, whose direction stands for the direction of active transport and the amplitude $|\mathbf{m}|$ for the strength of transport power. In the previous work [22], in which diffusion and concentration of auxin in tissue are assumed to be able to stimulate active transport, the notion of critical strength of active transport was introduced. Above this critical strength of active transport, cells are assumed to differentiate to form vessel segments. In our model, $|\mathbf{m}|$ can be viewed as playing a dual role: when the magnitude $|\mathbf{m}|$ is greater than some critical value m_0, we interpret this as the formation of a vascular segment, *i.e.*, the direction of $\mathbf{m}$ can be regarded as the direction of the segment and $|\mathbf{m}|^2$ as the conductance of the vascular segment.

The different means of transport can be modeled by the transport tensor,

$$\mathbf{A} = D\mathbf{I} + \tilde{\mathbf{A}} = D\mathbf{I} + \mathbf{m} \otimes \mathbf{m},$$

where D is the diffusion constant of the background substrate, $\mathbf{I}$ is the identity tensor, and $\otimes$ denotes the tensor product. Because the transport process is in general much faster than the initiation process, we can describe the transport process by the steady state equation

$$\nabla \cdot (\mathbf{A} \cdot \nabla P) = s, \tag{2.1}$$

where P is the partial pressure of the relevant hormone (*e.g.*, auxin) and s is the distribution of the source of hormone produced in the tissue. In general, the background diffusion constant is much smaller than the critical polarization power m_0^2. Therefore, for $|\mathbf{m}| > m_0$, Equation (2.1) can be effectively viewed as the Kirchoff's laws for obtaining the flow distribution in the vascular network. As will be discussed below, the distribution function s can be fluctuating. Then, the corresponding density of energy cost in transport becomes $\langle \nabla P \cdot \mathbf{A} \cdot \nabla P \rangle$, where $\langle \cdot \rangle$ is the average over all fluctuations. If the time scale of fluctuations is comparable to that of the transport, a non-steady-state transport equation should be used, which can lead to a reduction in the strength of fluctuations in flux.

Next, we consider the metabolic cost in forming a network. In comparison with pure diffusion, although active transport and flow in veins are more efficient in enhancing the delivery power and reducing the energy cost in transport, these two processes also require higher metabolic investment in maintaining high concentration of membrane proteins for active transport or in forming the veins and producing the fluid such as blood in the veins. In our model, we assume that the density of metabolic energy cost, $M(|\mathbf{m}|^2)$, can be effectively captured by a function of the amplitude of the polarization $\mathbf{m}$.

The total energy cost function can now be written as

$$E = \int_\Omega \left(\langle \nabla P \cdot \mathbf{A} \cdot \nabla P \rangle + M(|\mathbf{m}|^2) + \alpha |\nabla \mathbf{m}|^2 \right) dx,$$

where Ω is the tissue domain with x as the spatial coordinate. The term $\alpha|\nabla \mathbf{m}|^2$ takes into account the entropy associated with the intra- and inter-cellular diffusion of the polarization signal. A corresponding adaptation dynamics that fulfill the optimization principle can be modeled as follows by requiring that the total energy cost is decreasing along with the adaptation of the polarization vector $\mathbf{m}$:

$$\frac{\partial \mathbf{m}}{\partial t} = D_0 \triangle \mathbf{m} + c_0 (\langle (\mathbf{m} \cdot \nabla P) \nabla P \rangle - M'(|\mathbf{m}|^2)\mathbf{m}), \tag{2.2}$$

where D_0 is the diffusion constant of polarization signal, $c_0 = D_0/2\alpha$ is a constant that determines the time scale of adaptation. We use $\langle \cdot \rangle$ to represent the average of the stimuli over all fluctuating states. For $|\mathbf{m}| > m_0$, Equation (2.2) can be regarded as the corresponding adaptation process of the segments [14–16]. In other words, we have seamlessly integrated both the initiation process and the adaptation process of segments in a single model.

The adaptation dynamics of the polarization vector is dominated by the competition between two processes — the polarization process driven by the flux to enhance the delivery power and the natural contracting process to reduce the metabolic cost in maintaining the polarization or segments of the venation. At steady states of the adaptation dynamics, the total energy cost reaches a minimum and an optimal structure is obtained. It is worthwhile to point out that in our model the stimuli depend only on local information. This is important for living systems since communication of information is usually energetically costly.

Simulation results. Our model exhibits rich dynamics with a plethora of optimal structures. First, we consider the case of a fixed source (sink) distribution, namely, s is independent of time. As is shown by our simulation, the convexity of the metabolic cost function, $M(\cdot)$, plays a controlling role in the formation of the optimal structure. When $M(\cdot)$ is a concave function, the adaptation process induces the formation of a tree-like structure (see Figure 2.1); when it is convex, the steady state consists of a nearly uniform sheet without any vascular segment formation. The effects of convexity are consistent with the results obtained from discretized optimal transport networks [7, 8, 10, 11, 15]. For a concave metabolic cost function, intuitively, it is energetically favorable to deliver flow in concentrated channels instead of delivering separately through multiple parallel paths (a uniform sheet can be viewed as its limiting case). As a consequence, when the sources and sinks are fixed, loopy networks are unstable and tree-like structures emerge.

The diffusion constants, D and D_0, induce two characteristic length scales, *i.e.*, the characteristic length separating the smallest branches of a tree, l_0, and the characteristic width of veins, l_1. In particular, for a metabolic function in the form of power law, $M(|\mathbf{m}|^2) = b|\tilde{\mathbf{m}}|^{2\gamma}$, $\gamma < 1$, the two length scales become $l_0 = \sqrt{b\gamma D^{\gamma+1}}/s_0$ and $l_1 = \alpha^{\frac{1+\gamma}{4}} (b\gamma)^{-\frac{\gamma}{2}} D^{\frac{(1+\gamma)(1-\gamma)}{2}} s_0^{\frac{\gamma-1}{2}}$, respectively (see Appendix B). When the delivery length (the distance from a location to its nearest vascular segment) is much smaller than l_0, it is energetically favorable to transport directly by the background diffusion and there is no active transport, thus no formation of veins; in contrast, when the distance is much greater than l_0, active transport leads to the formation of veins so as to reduce the

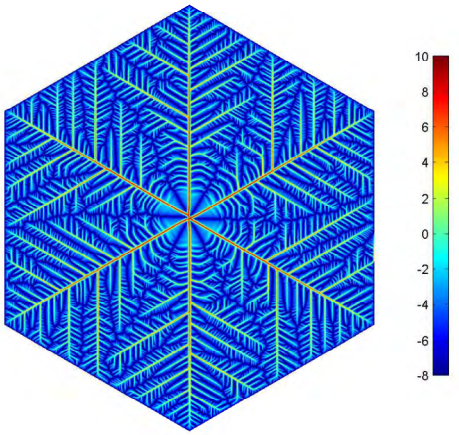

FIG. 2.1. *Optimal tree-like network structures obtained with the adaptation dynamics* (2.2). *Colors stand for the amplitude of* $\log(|\mathbf{m}|^2+D)$. *A uniform constant source* ($s=s_0$) *is fixed in the entire domain with a single sink at the center. The initial value of the polarization vector field is random and has the magnitude of the diffusion constant* $\sqrt{D}$. *The Neumann boundary conditions for Eqs.* (2.1) *and* (2.2) *are used in the simulation. Parameters:* $D=1\times10^{-3}$, $\alpha=1\times10^{-6}$, $c_0=5\times10^{-3}$, $b=1$, $s_0=1$, *and* $\gamma=0.5$. *The length of the hexagon edge is 1. See numerical methods in Appendix C.*

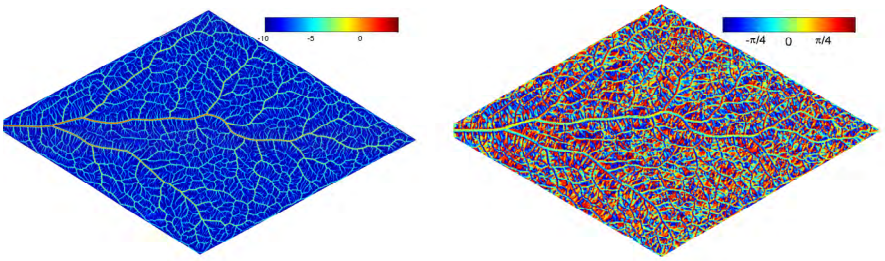

FIG. 2.2. *An optimal loopy network obtained with fluctuating sources. (a) Magnitude of the polarization vector filed. (b) Angle between the polarization vector and the x-axis, which shows that the polarization vector on an edge is approximately tangential to the edge. The domain is divided into 900 small sub-domains and the sources on only 10 randomly selected sub-domains are open at each time step. The Dirichlet boundary condition is applied for Equation* (2.1) *on the short edge on the left. All other boundary conditions are Neumann. Parameters:* $D=1\times10^{-6}$, $\alpha=1\times10^{-6}$, $c_0=5\times10^{-3}$, $b=1$, $s_0=1$, *and* $\gamma=0.5$. *The length of the diamond edge is 1.*

total energy cost. Therefore, l_0 characterizes the length between neighboring segments of the network. Meanwhile, l_1 characterizes the width of vascular segments. In the limiting case that both diffusion constants vanish, the steady-state network manifests a fractal structure.

Due to the concavity of the metabolic cost function, $M(\cdot)$, there is a large set of different optimal tree-like structures that can be obtained from different initial conditions of $\mathbf{m}$. Therefore, it is interesting to study how optimal networks with high energy cost can be avoided by the adaptation dynamics. According to our simulation, when the strength of the random initial polarization, $|\mathbf{m}|^2$, is much smaller than the background diffusion constant D, the optimal tree-like structures have similar appearances to each other; When the initial polarization is comparable to D, the configuration of optimal structures becomes sensitive to the initial value but the difference in total energy cost

between different optimal configurations is still small (*e.g.*, less than 3%); When the random initial polarization is significantly greater than D, the total energy cost of the optimal structures can be 10% greater than that obtained with small initial values. Therefore, we can control the background diffusion in the initiation process leading to optimal network structures with low energy cost. These simulation results suggest that high energy cost of locally optimal transport networks can be avoided by the adaptation dynamics with small initial value of the polarization, $\mathbf{m}$.

Loops are common in real biological transport networks. The question of how they arise and what benefit they can provide has attracted great interests [8, 9, 15, 17]. The benefit from loopy structures has been discussed on energy efficiency [8, 9, 15], damage tolerance [8], and mechanical robustness [17]. Theoretically, it was observed that loops become stable in a network as a result of fluctuations in flow distributions [15]. Interestingly, experimental observations also show that there are fluctuations in the production of auxin [19, 21, 26].

In order to study the effect of fluctuating sources, a Monte-Carlo method is used in our simulation: the tissue domain is divided into small sub-domains, and the hormone is produced only on a few randomly-selected sub-domains at each time step. With a sufficiently small time step, the adaptation process can also yield relatively stable networks. As is shown in Figure 2.2, loops are generated in the network through the adaptation dynamics when there is a small percentage of hormone-producing sub-domains at each step. From our simulation, the loop density (loop number per unit area) increases with the power parameter γ and decreases with the percentage of hormone-producing sub-domains at each step. In particular, when the percentage is greater than a critical value ($\sim$0.7 for $\gamma = 0.5$), no loops are found in the optimal network. Intuitively, a smaller power parameter γ means a more concave metabolic function, hence more unstable parallel pathways, thus more difficult to form stable loops. In contrast, a smaller percentage of hormone-producing sub-domains corresponds to stronger fluctuations in the flow distribution, thus making loops more stable. These results are consistent with the previous discussions on adaptation processes of discretized transport networks [15].

The above numerical results show that by incorporating sufficiently strong fluctuations in hormone sources, loops can spontaneously emerge along with the adaptation dynamics (2.2). From this point of view, fluctuations in hormone sources as observed in experiments may be employed simply to induce the formation of loops. With these loops, optimal vascular networks obtained from the adaptation dynamics (2.2) can meet well the requirement of network efficiency optimization under fluctuating flow demand.

Conclusion and discussion. We have proposed an optimization principle with its associated adaptation dynamics that integrates both the initiation and adaptation processes of general biological transport networks. The optimal structures are obtained at steady states of the adaptation dynamics. The adaptation dynamics is mainly driven by the competition between two local processes, which are required in structural optimization of the networks. The concavity of the metabolic cost function underlies the instability of parallel transport paths in the adaptation process and brings the network structures into being. For fixed sources (sinks), optimal networks possess tree-like structures due to the instability of parallel paths.

The background diffusion of hormone plays three important roles in the initiation process and also contributes in structural optimization. First, it spontaneously embeds the network into the tissue space. Second, it determines a characteristic length scale between neighboring segments. Below this length scale, pure diffusion incurs far less energy cost and there are no vascular segments or strong polarizations. Finally, with

pure diffusion, the initiation process can lead to an optimal network with low energy cost, since initial polarization is always small in life systems.

Fluctuations in the source production of hormones can change the instability of parallel pathways, leading to the formation of loops in networks. Since fluctuations in flow demand always exist in life systems, the physiological goal of the fluctuations in hormone production may be simply to achieve a loopy optimal vascular network. As has been discussed in the previous works [5, 15], the power exponent γ is equal to $1/2$ for blood vessel systems and the effective γ is greater than $1/2$ for leaf venation. This difference in the power exponent may underly the fact that most leaf venations have a larger loop density than arterial vessel systems, since loop density of optimal networks increases with the power exponent γ, as seen in our simulation.

The previous models on the adaptation and initiation processes of biological transport networks mostly start with a given prior initial network or cellular network structures [1, 6–13, 15, 20, 26–28]. In contrast to cellular models of the initiation of leaf venation [19–21], the anisotropic active transport is described by a polarization vector in our model. In our continuum model, networks embedded in given tissue geometry emerge spontaneously without requiring pre-given network or cellular structures. We note that the anisotropism is not responsible for the emergence of network, because scalar-based models and tensor-based models can also possess similar network structures (see Appendix A). The scalar-based model may be relevant to the emergence of network in slime mold *Physarum polycephalum* [1], where the conductivity for fluid delivery is isotropic.

In most cases, global optimization is not present in the designing of industrial transport networks. For industrial transport networks, although the objective function may be quite complex, it is still useful to separate it into the energy cost in delivery and energy cost in building the network. In particular, an adaptation process in response to local signals may still be useful to enhance the efficiency of the networks. Similar quantities may be introduced in designing these networks: For example, fluctuations in sources and sinks may be introduced to design loopy networks and enhance the efficiency and robustness of the networks; "background diffusion" may be introduced to embed the network into a two- or three-dimensional space and obtain optimal structures with low energy cost. Furthermore, space-dependent diffusion constant and source (sink) field may be employed flexibly to satisfy practical requirements in the designing of optimal industrial transport networks.

Acknowledgements. The work was supported by NSFC grants 11471213 and 91630208. This work was also supported by Center for High Performance Computing, Student Innovation Center, Shanghai Jiao Tong University, and the NYU Abu Dhabi Institute under grant G1301.

Appendix A. Scalar- and Tensor-based models.

A.1. Scalar-based model. The enhancement of transport power may be isotropic instead of direction-specific (*e.g.*, in the network emergence of slime mold *Physarum polycephalum*). Let $\tilde{A}$ be the enhancement of transport power, then the transport process is described by

$$\nabla\cdot\left(\left(\tilde{A}+D\right)\nabla P\right)=s, \tag{A.1}$$

where D is the diffusion constant and s is the source (sink) of flow or hormone. The adaptation dynamics of $\tilde{A}$ satisfies

$$\frac{\partial \tilde{A}}{\partial t} = D_0 \triangle \tilde{A} + c_0 \left(\langle \nabla P \cdot \nabla P \rangle - M' \left(\tilde{A} \right) \right), \tag{A.2}$$

where D_0 is the diffusion constant of the enhancement signal and c_0 is the parameter that determines the time scale of the adaptation dynamics. This adaptation dynamics satisfies the following energy relation

$$\begin{aligned} &\frac{d}{dt} \int_\Omega \left(\left(\tilde{A} + D \right) \langle |\nabla P|^2 \rangle + M(\tilde{A}) + \frac{D_0}{2c_1} |\nabla \tilde{A}|^2 \right) dx \\ =& -\frac{1}{c_0} \int_\Omega \left(D_0 \triangle \tilde{A} + c_0 \left(\langle |\nabla P|^2 \rangle - M' \left(\tilde{A} \right) \right) \right)^2 dx. \end{aligned}$$

Thus the adaptation dynamics lead to the formation of optimal transport network.

A.2. Tensor-based model. Similarly, we construct the tensor-based model. Let $\tilde{\mathbf{A}}$ represent the polarization tensor of transport power due to active transport or transport in veins. We define the transport tensor as $\mathbf{A} = D\mathbf{I} + \tilde{\mathbf{A}}$. The transport process can be described by

$$\nabla \cdot (\mathbf{A} \cdot \nabla P) = s. \tag{A.3}$$

The adaptation dynamics of $\tilde{\mathbf{A}}$ satisfies

$$\frac{\partial \tilde{\mathbf{A}}}{\partial t} = D_0 \triangle \tilde{\mathbf{A}} + c_0 (\langle \nabla P \otimes \nabla P \rangle - M'(|\tilde{\mathbf{A}}|) \frac{\tilde{\mathbf{A}}}{|\tilde{\mathbf{A}}|}), \tag{A.4}$$

where $|\tilde{\mathbf{A}}|$ is the Frobenius norm of $\tilde{\mathbf{A}}$. This system of equations satisfies the following energy relation

$$\begin{aligned} &\frac{d}{dt} \int_\Omega \left(\langle \nabla P \cdot \mathbf{A} \cdot \nabla P \rangle + M(|\tilde{\mathbf{A}}|) + \frac{2D_0}{2c_1} |\nabla \tilde{\mathbf{A}}|^2 \right) dx \\ =& -\frac{1}{c_1} \int_\Omega \left| D_0 \triangle \tilde{\mathbf{A}} + c_1 (\langle \nabla P \otimes \nabla P \rangle - M'(|\tilde{\mathbf{A}}|) \frac{\tilde{\mathbf{A}}}{|\tilde{\mathbf{A}}|}) \right|^2 dx. \end{aligned}$$

In the tensor-based model, we do not distinguish between the positive and negative direction of the active transport. In the adaptation dynamics, a newly formed vessel segment can lead to redistribution of polarizations in the neighboring tissue, including the change of direction of the active transport. For the vector based model in the main text, the directional change can only be achieved by a rotation of the polarization vector; For the tensor-based model, it can be achieved by changing the principle eigenvector of the polarization tensor; in contrast, for the scalar-based model, there is no need of directional change. The latter two are relatively easy to achieve. As a result, the adaptation dynamics of the scalar- and tensor-based models can find transport networks with less energy cost than that obtained from the vector-based model (a network obtained with the tensor-based model is shown in Figure A.1). However, the energy cost of the networks obtained from different models is not significant.

Appendix B. Dimensional analysis of the length scales.

For the characteristic length separating the smallest branches of a tree, l_0, we note that over this length scale, the efficiency of pure diffusion is comparable to the active transport. Thus by nondimensionalizing the first equation in the main text, we have

$$D \sim m_0^2, \text{ and } D \frac{P_0}{l_0^2} \sim s_0,$$

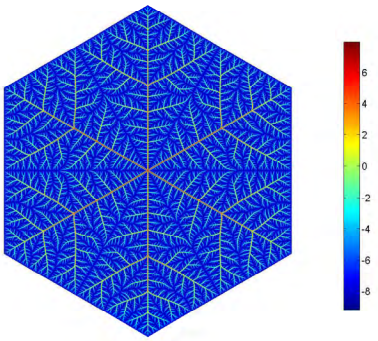

FIG. A.1. *Optimal tree-like network structure obtained with the tensor-based model. Colors stand for the amplitude of* $\log\left(|\tilde{A}|+D\right)$. *A uniform constant source* ($s=s_0$) *is fixed in the entire domain with a single sink at the center. The initial value of the polarization tensor is random and has the magnitude of the diffusion constant* $\sqrt{D}$. *The Neumann boundary conditions are used in the simulation. Parameters:* $D=1\times10^{-4}$, $\alpha=1\times10^{-6}$, $c_0=5\times10^{-3}$, $b=1$, $s_0=1$, *and* $\gamma=0.5$. *The length of the hexagon edge is 1.*

where P_0 and m_0 are the characteristic scale of P and $\mathbf{m}$ away from the veins, respectively. Noting that the terms in the bracket of Equation (2.2) should almost cancel each other out, we have

$$m_0\frac{P_0^2}{l_0^2}\sim\gamma b m_0^{2\gamma-1}.$$

By cancelling P_0 and m_0, we obtain the characteristic length separating the smallest branches of the tree, $l_0=\sqrt{b\gamma D^{1+\gamma}}/s_0$.

For the characteristic width of veins, we may consider the smallest veins since the change of the width is not significant. From Equation (2.1), the flux in the veins satisfies

$$m_1^2 P_d l_1\sim s_0 l_0^2,$$

where m_1 is the characteristic scale of $\mathbf{m}$ in the veins and P_d is the characteristic scale of ∇P along the direction of the veins. Noting that the three terms on the right-hand side of Equation (2.2) should be of the same magnitude in the veins at steady state, we obtain

$$\alpha\frac{m_1}{l_1^2}\sim m_1 P_d^2\sim b\gamma m_1^{2\gamma-1}.$$

By cancelling m_1 and P_d, we obtain $l_1=\alpha^{\frac{1+\gamma}{4}}(b\gamma)^{-\frac{\gamma}{2}}D^{\frac{(1+\gamma)(1-\gamma)}{2}}s_0^{\frac{\gamma-1}{2}}$.

Appendix C. Brief description of the numerical methods. The standard finite element method can be used to solve the equation for the steady-state transport process (1). The PDE-toolbox in matlab can be employed to solve this equation at each time step.

Note that the diffusion constant D_0 is very small in general. As a result, the explicit finite difference method can be directly employed to solve the evolution Equation (2.2). In our simulation, since the triangle mesh is used to solve the system, an operator-splitting method is used to solve the evolution equation: the heat kernel is used to update the the diffusion part of the equation, whereas the Euler method is used to update the nonlinear part.

REFERENCES

[1] A. Tero, S. Takagi, T. Saigusa, K. Ito, D. Bebber, M. Fricker, K. Yumiki, R. Kobayashi, and T. Nakagaki, *Rules for biologically inspired adaptive network design*, Science, 327:439–442, 2010. 1, 2

[2] A. Tero, T. Nakagaki, K. Toyabe, K. Yumiki, and R. Kobayashi, *A method inspired by physarum for solving the Steiner problem*, Int. J. Unconv. Comput., 6(2):109–123, 2010. 1

[3] M. Goemans and Y. Myung, *A catalog of Steiner tree formulations*, Networks, 23:19–28, 1993. 1

[4] R. Thoma, *Untersuchungen uber die Histogenese und Histomechanik des Blutgefasssystems*, Stuttgart: Enke Verlag, 1893. 1

[5] C. Murray, *The physiological principle of minimum work. I. The vascular system and the cost of blood volume*, Proc. Natl. Acad. Sci. USA, 12(3):207–214, 1926. 1, 2

[6] T. Nelson and N. Dengler, *Leaf vascular pattern formation*, Plant Cell, 9:1121–1135, 1997. 1, 2

[7] S. Bohn and M. Magnasco, *Structure, scaling, and phase transition in the optimal transport network*, Phys. Rev. Lett., 98:088702, 2007. 1, 2, 2

[8] E. Katifori, G. Szollosi, and M. Magnasco, *Damage and fluctuations induce loops in optimal transport networks*, Phys. Rev. Lett., 104:048704, 2010. 1, 2, 2, 2

[9] F. Corson, *Fluctuations and redundancy in optimal transport networks*, Phys. Rev. Lett., 104:048703, 2010. 1, 2, 2

[10] J. Banavar, F. Colaiori, A. Flammini, A. Maritan, and A. Rinaldo, *Topology of the fittest transportation network*, Phys. Rev. Lett., 84:4745, 2000. 1, 2, 2

[11] M. Durand, *Structure of optimal transport networks subject to a global constraint*, Phys. Rev. Lett., 98:088701, 2007. 1, 2, 2

[12] M. Durand, *Architecture of optimal transport networks*, Phys. Rev. E, 73:016116, 2006. 1, 2

[13] D. Hu, D. Cai, and A. Rangan, *Blood vessel adaptation with fluctuations in capillary flow distribution*, PLoS One, 7(9):e45444, 2012. 1, 2

[14] Q. Chen, L. Jiang, C. Li, D. Hu, J. Bu, D. Cai, and J. Du, *Haemodynamics-driven developmental pruning of brain vasculature in zebrafish*, PLoS Biol., 10(8):e1001374, 2012. 1, 2

[15] D. Hu and D. Cai, *Adaptation and optimization of biological transport networks*, Phys. Rev. Lett., 111:138701, 2013. 1, 2, 2, 2, 2

[16] T. Secomb, J. Alberding, R. Hsu, M. Dewhirst, and A. Pries, *Angiogenesis: an adaptive dynamic biological patterning problem*, PLoS Comput. Biol., 9(3):e1002983, 2013. 1, 2

[17] M. Laguna, S. Bohn, and E. Jagla, *The role of elastic stresses on leaf venation morphogenesis*, PLoS Comput. Biol., 4:e1000055, 2008. 1, 2

[18] E. Jones, F. Noble, and A. Eichmann, *What determines blood vessel structure? Genetic prespecification vs. hemodynamics*, Physiology, 21:388–395, 2006. 1

[19] O. Avsian-Kretchmer, J. Cheng, L. Chen, E. Moctezuma, and R. Sung, *Indole acetic acid distribution coincides with vascular differentiation pattern during Arabidopsis leaf ontogeny*, Plant Physiol., 130:199–209, 2002. 1, 2, 2, 2

[20] J. Mattsson, R. Sung, and T. Berleth, *Responses of plant vascular systems to auxin transport inhibition*, Development, 126:2979–2991, 1999. 1, 2, 2

[21] L. Sieburth, *Auxin is required for leaf vein pattern in Arabidopsis*, Plant Physiol., 121:1179–1190, 1999. 1, 2, 2, 2

[22] P. Dimitrov and S. Zucker, *A constant production hypothesis guides leaf venation patterning*, Proc. Natl. Acad. Sci. USA, 103:9363–9368, 2006. 1, 2

[23] R. Merks, S. Brodsky, M. Goligorksy, S. Newman, and J. Glazier, *Cell elongation is key to in silico replication of in vitro vasculogenesis and subsequent remodeling*, Dev. Biol., 289:44-54, 2006. 1

[24] L. Lamalice, R. Boeuf, and J. Huot, *Endothelial cell migration during angiogenesis*, Circ. Res., 100:782–794, 2007. 1

[25] T. Sachs, *The control of the patterned differentiation of vascular tissues*, Adv. Bot. Res., 9:151–262, 1981. 1

[26] G. Mitchison, *A model for vein formation in higher plants*, Proc. Roy. Soc. B, 207:79–109, 1980. 1, 2, 2

[27] T. Sachs, *Collective specification of cellular development*, BioEssays, 25:897–903, 2003. 1, 2

[28] A. Rolland-Lagan, and P. Prusinkiewicz, *Reviewing models of auxin canalization in the context of leaf vein pattern formation in Arabidopsis*, Plant J., 44:854–865, 2005.

1, 2